On the occurrence of chaos in a parametrically driven extended Rayleigh oscillator with three-well potential

M. Siewe Siewe [a], Hongjun Cao [b,c], Miguel A.F. Sanjuán [c,*]

[a] *Laboratoire de Mécanique, Département de Physique, Faculté des Sciences, Université de Yaoundé I, B.P. 812 Yaoundé, Cameroon*
[b] *Department of Mathematics, School of Science, Beijing Jiaotong University, Beijing 100044, PR China*
[c] *Nonlinear Dynamics and Chaos Group, Departamento de Física, Universidad Rey Juan Carlos, Tulipán s/n,*
28933 Móstoles, Madrid, Spain

Abstract

We examine the chaotic behavior of an extended Rayleigh oscillator in a three-well potential under additive parametric and external periodic forcing for a specific parameter choice. By applying Melnikov method, we obtain the condition for the existence of homoclinic and heteroclinic chaos. The numerical solution of the system using a fourth-order Runge–Kutta method confirms the analytical predictions and shows that the transition from regular to chaotic motion is often associated with increasing the energy of an oscillator. An analysis of the basins of attraction showing fractal patterns is also carried out.
© 2008 Elsevier Ltd. All rights reserved.

1. Introduction

This paper is concerned with the appearance of homoclinic and heteroclinic instabilities and chaos in a triple-well oscillator studied by Li and Moon [1]. Many problems in physics, chemistry, biology, etc., are related to nonlinear self-excited oscillators [2]. For example, the self-excited oscillations in bridges and airplane wings, the beating of a heart, and the nonlinear model of a machine tool chatter [6]. A self-excited oscillator is a system which has some external source of energy upon which it can be drawn. Self-excited systems have a long history in the field of mechanics [7,8]. One of its most prominent features is the existence of stable limit cycles in phase space, emerging from a balance between the energy gain and the dissipation. Another feature is their instabilities. Recently, self-excited systems have been proposed as fundamental tools for control and reduction of friction [9–11]. The possible influence of self-excited dynamics on friction force is based on the idea that when a limit cycle is established, then limited changes of external conditions cannot destroy it and the system persists on its frictionless oscillating motion.

Parametric perturbations are characterized by parameters periodically in time changing and they are described by homogeneous differential equations of motion. Many works on self-excited, parametrically and externally excited are well known and deeply investigated in the literature separately. Minorski [12] is one of the first authors considering

* Corresponding author.
 E-mail address: miguel.sanjuan@urjc.es (M.A.F. Sanjuán).

the interaction between two different types of perturbations. Warminski [14] emphasizes the differences in modelling ideal and non-ideal systems for a chosen class of self-excited, parametric and externally excited vibrations. Many of those studies lead to the parametric excitation combined with self-excited system and subjected to an external force which quite often take the form

$$\ddot{x} + \eta(x, \dot{x})\dot{x} + (1 - \mu\cos 2\omega t)(x + \alpha x^3) = F\cos\omega t, \tag{1}$$

where $(x, \dot{x})$ is a nonlinear damping function. The effect of nonlinear damping on a nonlinear oscillator was investigated previously in Ref. [13], showing among other things how it affected the evolution of fractalization of phase space. The effect of nonlinear dissipation on the boundaries of basin of attraction in a two-well Rayleigh–Duffing oscillator was also analyzed in detail in Ref. [26]. Eq. (1) can be seen as a model describing the dynamics of a mass-spring damper system with the nonlinear damping and where the restoring force is an anharmonic function in which the parameters vary with time. This model have been studied intensively in Refs. [14–17], where new dynamical phenomena have been found; for example, interactions between parametric and self-excited vibrations lead to quasi-periodic motion. However, in the neighborhood of parametric resonances, the system synchronizes, and after the inverse secondary Hopf's bifurcation, the motion becomes periodic. Even though most perturbations applied to the system are harmonic, the effect of considering non-harmonic perturbations was also considered in [28,29]. In 1965, an interesting paper appeared where Wehrmann [18] was able to suppress turbulence behind a cylinder in a moving fluid. The basic idea was to put the cylinder in vibration with a suitable feed-back using the same fluctuations presented in the turbulent fluid. A complete laminarization was obtained. Turbulence is a kind of phenomenon related to a system with infinite degrees of freedom and it is natural to wonder if parametric perturbations can modify the onset of chaos in low dimensional system as well. The authors in Refs. [19,20] showed with a rigorous theoretical consideration that the resonant parametric perturbation can remove chaos in low dimensional systems. They confirmed this prediction with numerical simulations. Furthermore, Cicogna [21] showed, using the Melnikov analysis [22], how to modify the threshold of chaos by resonant parametric modulation. Another good example is constituted by the generalized perturbed pendulum [31].

In contrast to the Rayleigh–Duffing oscillator (see Eq. (1)), the investigation of Eq. (1) including fifth nonlinearities in the restoring forced has not received much attention. Nevertheless, some attention has deserved the analysis of a three-well potential and the Rayleigh oscillator itself quite recently [3–5]. It is interesting to note that there is a situation analyzed in [27], where Melnikov analysis is applied to a nonlinear oscillator which can behave as a one-well oscillator or a two-well oscillator by simply modifying one of its parameters, which acts as a symmetry-breaking mechanism. Therefore, the chaotic behavior using the parametric perturbation in the modified Rayleigh–Duffing oscillator with a three-well potential still needs to be investigated further. The model Eq. (1), which includes the cubic (x^3) and quintic (x^5) terms, and in the absence of parametric excitation (i.e. $\mu = 0$) was used to study the motions of the platform of a ski-simulator [23].

In the present work we focus our attention on the study of the effects of parametric periodic excitation on the fractal basin boundaries of a three-well potential of an extended Rayleigh–Duffing oscillator possessing both homoclinic and heteroclinic orbit.

The rest of the paper is organized as follows. In Section 2, we briefly give the description of the model and we find the local bifurcation of the unperturbed system. In Section 3, the conditions of existence of Melnikov's chaos under parametric perturbation resulting from the homoclinic and heteroclinic bifurcation are performed. Finally in Section 4, a convenient demonstration of the accuracy of the method is obtained from the fractal basin boundaries. We end in Section 5 with conclusions.

2. Description of the model and analysis of the unperturbed system

2.1. Description of the model

In this paper, we examine the dynamical transitions in parametric and periodically forced self-oscillating systems containing the cubic and quintic terms in the restoring force as follows:

$$\dot{x} = y, \quad \dot{y} = -(-a + b\dot{x}^2)\dot{x} - (1 - \mu\cos 2\omega t)(x + \alpha x^3 + \beta x^5) + F\cos\omega t, \tag{2}$$

where a, b, μ, α, β, F and ω are parameters. Physically, a and b represent respectively linear and nonlinear damping coefficient terms, μ and F are the amplitudes of the parametric and external periodic forcing, and ω is the corresponding frequency. Moreover α and β characterizes the intensity of the nonlinearity. The equation describes self-excited oscillations for $a > 0$ and $b > 0$. This equation is a mixed type of Rayleigh and the modified Duffing oscillator.

2.2. Analysis of the unperturbed system

In this subsection, we derive the fixed points and the phase portrait corresponding to the system Eq. (2) when it is unperturbed. If we let $a = b = \mu = F = 0$, Eq. (2) is considered as an unperturbed system and can be rewritten as

$$\dot{x} = y, \quad \dot{y} = -x - \alpha x^3 - \beta x^5. \tag{3}$$

The system of Eq. (3) corresponds to an integrable Hamiltonian system with a potential function

$$V(x) = \frac{1}{2}x^2 + \frac{\alpha}{4}x^4 + \frac{\beta}{6}x^6, \tag{4}$$

and the associated Hamiltonian function is given by

$$H(x,y) = \frac{1}{2}y^2 + \frac{1}{2}x^2 + \frac{\alpha}{4}x^4 + \frac{\beta}{6}x^6. \tag{5}$$

From Eqs. (3) and (5), we can compute the fixed points and analyze their stabilities.

(i) For $\alpha^2 < 4\beta$, there is one fixed point $(0,0)$ which is a center. If $\beta > 0$, the potential given by Eq. (4) has only a single-well. If $\beta < 0$, it has only a single-well symmetric potential.

(ii) For $\alpha > 0, \beta < 0$, with $\alpha^2 > 4\beta$, there are three fixed points: two saddles connected by two heteroclinic orbits and one center.
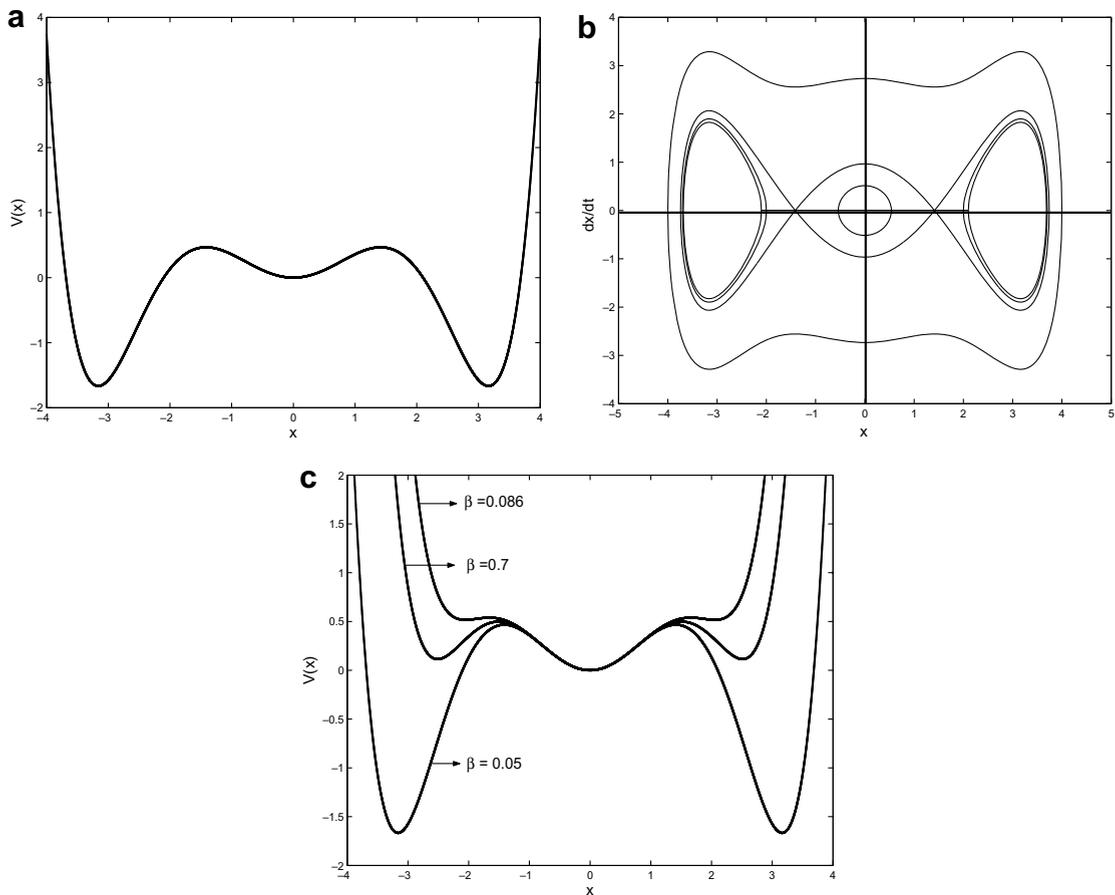

Fig. 1. (a) Three-well potential function given by $V(x) = 0.5x^2 - 0.15x^4 + 1/120x^6$. (b) Corresponding phase portraits. (c) Shape of three-well potential function $V(x) = 0.5x^2 - 0.15x^4 + \beta/6x^6$ for different values of β.

(iii) For $\alpha < 0, \beta > 0$, with $\alpha^2 > 4\beta$, there are five fixed points: two saddles connected by two heteroclinic orbits, and the two saddle points are connected to themselves by one homoclinic orbit. In addition, there are three centers.

Since we are interested in the case of a three-well potential, this corresponds to the case (iii), and then we fix the parameter values to be $\alpha = -0.6$, $\beta = 0.05$ throughout this paper. The phase portrait and the potential function of the system given by Eq. (3) are shown in Fig. 1a and b, respectively. In Fig. 1c it can be observed how the shape of the potential function varies for different values of β.

3. Horseshoe chaos for damped and periodic perturbation

We now suppose that the unperturbed system discussed in the previous section is perturbed by a combination of dissipative $(-a + b\dot{x}^2)\dot{x}$, periodic $(F \cos \omega t)$ forces, and parametric forces $(\mu \cos 2\omega t)$ and take a, b, μ, and F to be small parameters where μ, and $F \ll 1$. We will investigate theoretically the condition for the onset of homoclinic and heteroclinic behavior by applying the Holmes–Melnikov method to Eq. (2). A transformation of $a \to \varepsilon a$, $b \to \varepsilon b$, $\mu \to \varepsilon \mu$, $F \to \varepsilon F$ is done in order to apply the ε first-order perturbation of ε of the Holmes–Melnikov method. Hence, the horseshoe chaos for our model equation is analyzed by transforming Eq. (2) into a system of the first-order differential equation of the following form

$$
\begin{cases}
\dot{x} = y, \\
\dot{y} = -x - \alpha x^3 - \beta x^5 - \varepsilon((-a + b\dot{x}^2)\dot{x} - \mu(x + \alpha x^3 + \beta x^5)\cos \phi_1 - F \cos \phi_2), \\
\dot{\phi}_1 = 2\omega, \\
\dot{\phi}_2 = \omega.
\end{cases}
\tag{6}
$$

The unperturbed system for system Eq. (6) (i.e. $\varepsilon = 0$) has two homoclinic orbits and one heteroclinic orbit as shown in Fig. 1b. When the perturbations are added, the closed homoclinic or heteroclinic orbits break, and may have transverse homoclinic or heteroclinic orbits. By using the Smale–Birkhoff Theorem [30], the existence of such orbits results in chaotic dynamics. As is well-known, the Melnikov method provides the estimates in parameter space for the appearance of homoclinic (and heteroclinic) bifurcations, and hence for transient chaos. This means that in most cases only the necessary conditions for steady chaos (strange chaotic attractor) are obtained from the method. Therefore, one may always get sufficient conditions for the inhibition of even transient chaos (frustration of homoclinic/heteroclinic bifurcation) and, a fortiori, for the inhibition of the steady chaos that ultimately arises from such a homoclinic/heteroclinic bifurcation. In their previous work, Siewe et al. [24,25] has showed that when $\varepsilon = 0$, the system Eq. (6) is a Hamiltonian system with a pair of heteroclinic orbits defined as follows:

$$
(x_h^{\pm}, (y_h)^{\pm}) = \left(\pm \frac{x_1\sqrt{2}\sinh\left(\frac{T_1 t}{2}\right)}{\sqrt{-\xi + \cosh(T_1 t)}}, \pm \frac{T_1 x_1 \sqrt{2}(1-\xi)\cosh\left(\frac{T_1 t}{2}\right)}{2(-\xi + \cosh(T_1 t))^{3/2}} \right)
\tag{7}
$$

and possesses a pair of symmetric homoclinic trajectories connecting each unstable point to itself given by

$$
(x_h^{\pm}, (y_h)^{\pm}) = \left(\pm \frac{x_1\sqrt{2}\cosh\left(\frac{T_1 t}{2}\right)}{\sqrt{\xi + \cosh(T_1 t)}}, \mp \frac{T_1 x_1 \sqrt{2}(1-\xi)\sinh\left(\frac{T_1 t}{2}\right)}{2(\xi + \cosh(T_1 t))^{3/2}} \right),
\tag{8}
$$

where $T_1 = x_1^2\sqrt{2\beta(\theta^2 - 1)}$; $A^2 = x_2^2(\theta^2 + 3)$; $\xi = \frac{5 - 3\theta^2}{3\theta^2 - 1}$; $\theta^2 = \frac{\alpha - \sqrt{\alpha^2 - 4\beta}}{\alpha + \sqrt{\alpha^2 - 4\beta}}$.

According to Eq. (7) and (8), the signs refer to the right and left half planes. Both solutions determine the separatrix orbit, since it separates two types of orbits in phase space + refers to the hetero/homoclinic trajectory with $x > 0$ and − refers to the hetero/homoclinic trajectory with $x < 0$. We therefore apply the Melnikov method to system Eqs. (6) for finding the criteria of the existence of homoclinic or heteroclinic bifurcation and chaos.

$$
M^{\pm}(t_0) = a \int y_h^2 \, dt - b \int y_h^4 \, dt - \mu \int x_h y_h \cos 2\omega(t - t_0) \, dt + F_0 \int y_h \cos \omega(t - t_0) \, dt + \mu\alpha \int x_h^3 y_h \cos 2\omega(t - t_0) \, dt
$$
$$
+ \mu\beta \int x_h^5 y_h \cos 2\omega(t - t_0) \, dt,
\tag{9}
$$

where t_0 is the cross-section time of the Poincaré map and t_0 can be interpreted as the initial time of the forcing term. This Melnikov expression comprises in a compact way a lot of particular results that can be found in the literature.

3.1. Heteroclinic bifurcation

Let us first consider the case of heteroclinic orbit. It has been shown that three singular points, given by $x_1^{\pm}$ which are saddles, and $x_0 = (0,0)$ which is a center. The zero solution bifurcates into a family of limit cycles which are stable. Inside the left and right region of Fig. 1b, there exist two limit cycles. Substituting the heteroclinic solution given by Eq. (7) into the Melnikov function given by Eq. (9) which need to be evaluated, it appears that the Melnikov function for the heteroclinic orbits is given by

Fig. 2. Heteroclinic bifurcation curves in the (ω, μ_{he}) plane when varies the external forced: (solid line) $F = 0.1$ (dash line) $F = 0.05$ (dot line) $F = 0.01$ the others parameters are $a = 0.012$, $b = 0.0002$.
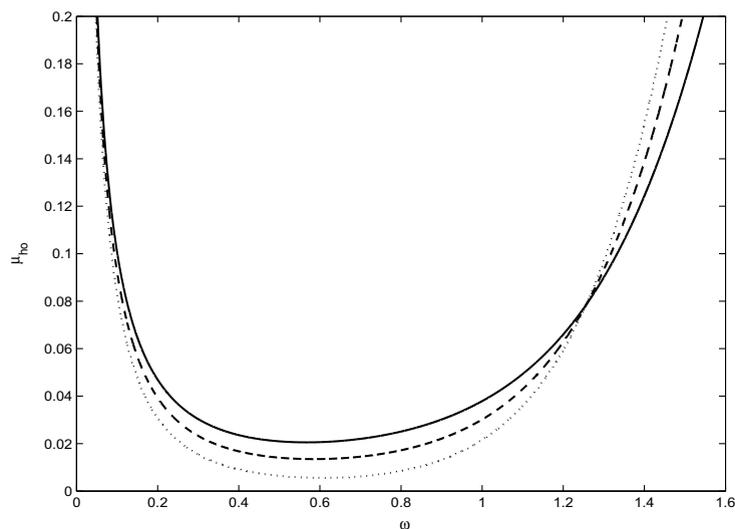

Fig. 3. Homoclinic bifurcation curves in the (ω, μ_{he}) plane when varies the external forced: (solid line) $F = 0.2$ (dash line) $F = 0.1$ (dot line) $F = 0.01$ the others parameters are $a = 0.012$, $b = 0.01$.

$$M^+(t_0) = \frac{x_1^2 T_1}{2(1+\xi)} \left[a(\xi+2) + \frac{bx_1^2 T_1^2 C_{\text{he}}}{160(1+\xi)^3} + \frac{\arcsin\xi + \frac{\pi}{2}}{\sqrt{1-\xi^2}} \left[a(1+2\xi) + \frac{bx_1^2 T_1^2 D_{\text{he}}}{160(1+\xi)^3} \right] \right]$$

$$+ \frac{4\mu x_1^2 \omega^2}{T_1^2 \sinh\frac{2\pi\omega}{T_1}} \left(2\pi + \frac{\pi\alpha x_1^2}{3} \left(5 - \frac{4\omega^2}{T_1^2} \right) + \frac{2\beta x_1^4 \eta_2}{3} \right) \sin 2\omega t_0 + \frac{2\pi\omega F x_1}{T_1 \sinh\frac{\pi\omega}{T_1}} \cos \omega t_0. \qquad (10)$$

It follows from the Melnikov theory that, to keep the heteroclinic loop preserved under a perturbation, it is necessary and sufficient that $M^+(t_0) \equiv 0$ and $\frac{dM^\pm}{dt} \neq 0$ at $t = t_0$. Thus, a bifurcation curve for the heteroclinic bifurcation can be solved from Eq. (10) as

$$\mu \geqslant \mu_{\text{he}} = \left| \left(1 - \frac{R_1}{R_3} \right) R \right|, \qquad (11)$$

which implies that if $\varepsilon > 0$ is sufficiently small, the reduced Eq. (6) has transverse heteroclinic orbits resulting in the possible chaotic dynamic.

By Melnikov analysis given by Eq. (10), Fig. 2 shows the critical values for heteroclinic bifurcation μ_{he} as functions of frequency ω under the action of a harmonic excitation. One can see that when the value of the harmonic excitation F increases, the thresholds of μ_{he} increase. It is also found that for a fixed value of the harmonic excitation, there are two
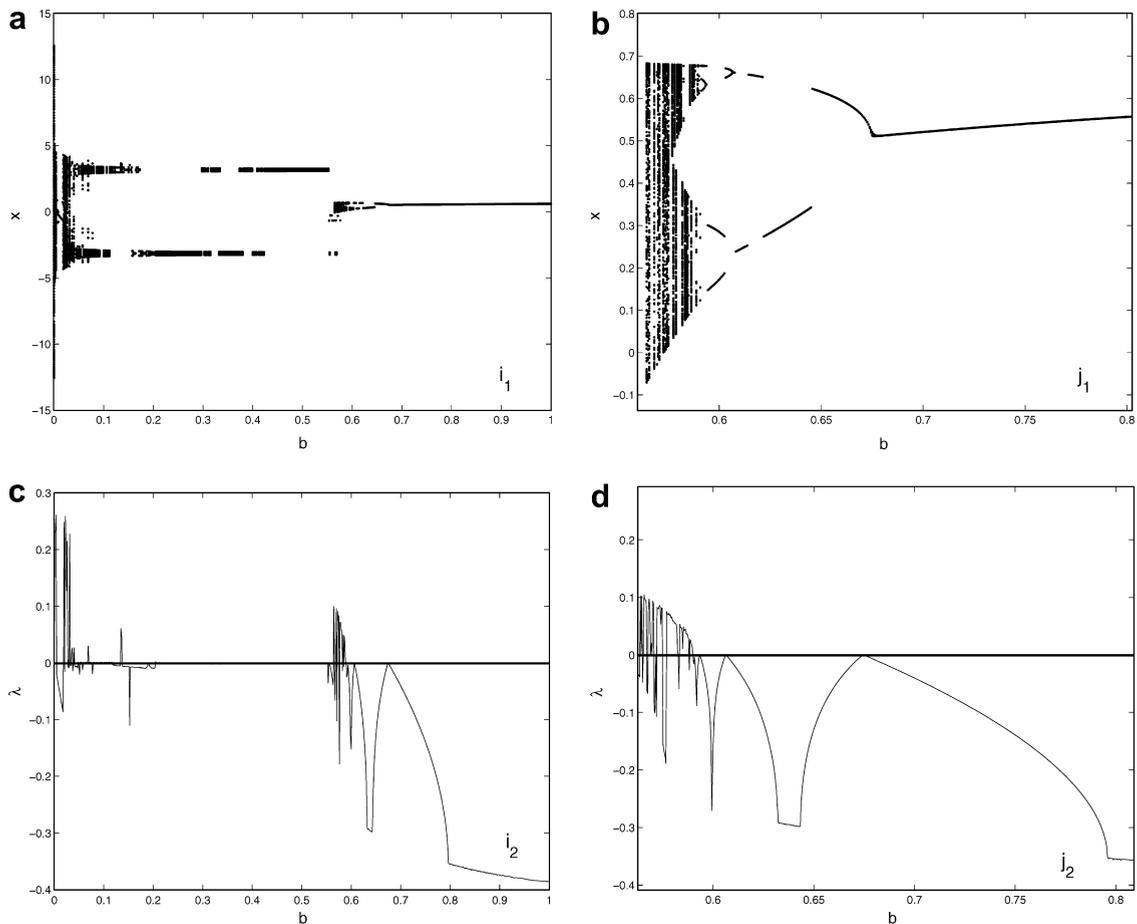

Fig. 4. (a) Bifurcation diagram of the equation $\ddot{x} + (-0.012 + 0.0002\dot{x}^2)\dot{x} + (1 - 0.85\cos 1.5t)(x - 0.6x^3 + 0.05x^5) = 0.01\cos 0.75t$ in the (b,x) plane for $x \in [0,1]$ with $(x_0, \dot{x}_0) = (0.1, 0.5)$. (b) Maximum Lyapunov exponent corresponding to (a). (c) Bifurcation diagram of the equation $\ddot{x} + (-0.012 + 0.0002\dot{x}^2)\dot{x} + (1 - 0.85\cos 1.5t)(x - 0.6x^3 + 0.05x^5) = 0.01\cos 0.75t$ for $x \in [0.52, 0.8]$ showing the transition from chaos to the period doubling and to the period-one. (d) Maximum Lyapunov exponent corresponding to (b) showing the transition from chaos to the periodic region.

critical values under which heteroclinic bifurcation may occur. This can be due to the effect of the strongly nonlinearities in our model Eq. (2)

3.2. Homoclinic bifurcation

Now consider the case of homoclinic orbit and substituting Eq. (8) into Eq. (9) and evaluating the integral, we obtain the Melnikov function

$$
M^{\pm}(t_0) = \frac{x_1^2 T_1}{4(1+\xi)^2} \left[a(\xi^2 + 3\xi - 2) + \frac{bx_1^2 T_1^2 C_{\text{ho}}}{120(1+\xi)^2} + \frac{\arcsin \xi - \frac{\pi}{2}}{\sqrt{1-\xi^2}} \left[a\xi(3\xi - 1) + \frac{bx_1^2 T_1^2 D_{\text{ho}}}{120(1+\xi)^2} \right] \right]
$$
$$
- \frac{2\pi\mu x_1^2 \omega}{T_1 \sinh \frac{2\pi\omega}{T_1}} \left[\frac{\sinh\left(\frac{2\omega}{T_1} \arccos \xi\right)}{\sqrt{1-\xi^2}} + \frac{4\alpha x_1^2 \omega^2(1-\xi)\eta_3}{3T_1(1+\xi)^2} + \frac{4\beta\omega^2 x_1^4(1-\xi)\eta_4}{15T_1(1+\xi)^3} \right] \sin 2\omega t_0 - \frac{2Fx_1}{T_1} \sin \frac{2\omega}{T_1}
$$
$$
\times \sin \omega t_0. \tag{12}
$$

Since the Melnikov function theory measures the distance between the perturbed stable and unstable manifolds in the Poincaré section, to preserve the homoclinic loops under a perturbation requires that at t_0, if $M(t_0)^{\pm}$ has a simple zero, then a homoclinic bifurcation occurs, signifying the possibility of chaotic behavior. This means that only necessary conditions for the appearance of chaos are obtained from Poincaré–Melnikov–Arnold analysis, and therefore one always has the chance of finding sufficient conditions for the elimination of even transient chaos. The necessary condition for which the invariant manifolds intersect is given by

$$
\mu \geqslant \mu_{\text{ho}} = \left| \left(1 - \frac{K_1}{K_3}\right) K \right|, \tag{13}
$$

which implies that if $\varepsilon > 0$ is sufficiently small, the reduced Eq. (5) has transverse homoclinic orbits resulting in the possible chaotic dynamics.
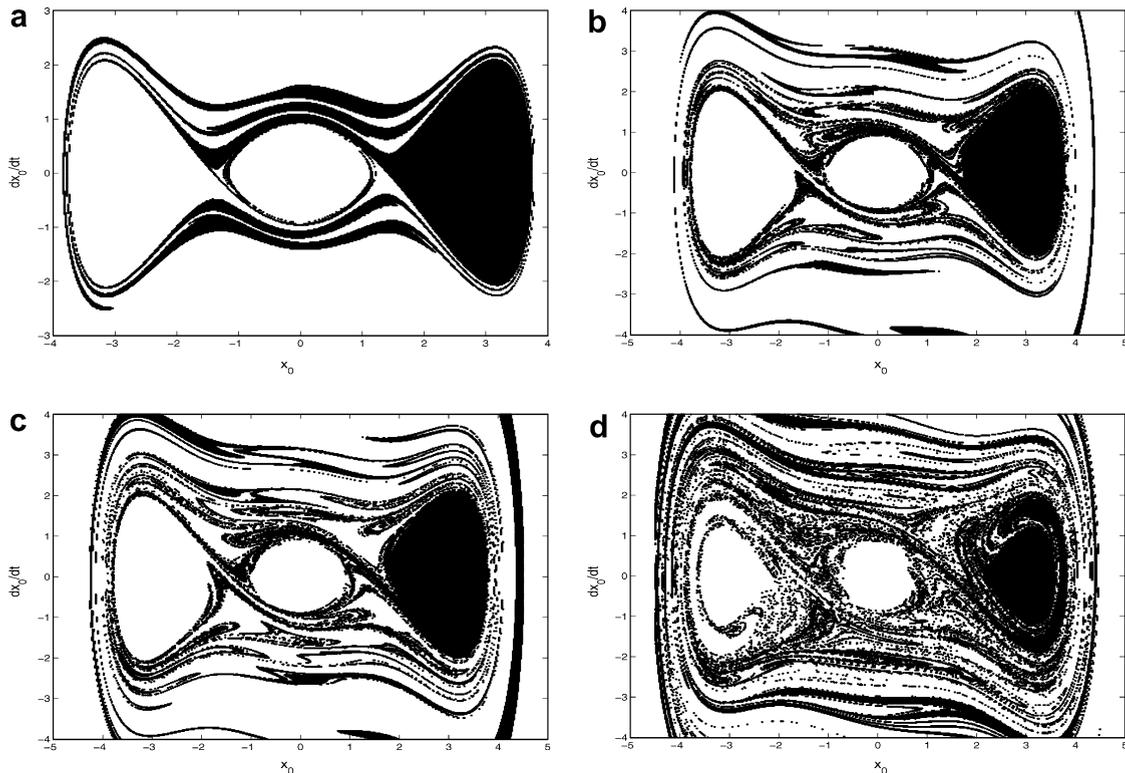

Fig. 5. Basin of attraction inside the right-hand potential well: (a) $\mu_{\text{ho}} = 0.01$, (b) $\mu_{\text{ho}} = 0.09$, (c) $\mu_{\text{ho}} = 0.13$ and (d) $\mu_{\text{ho}} = 0.3$, the others parameters are: $F = 0.01$, $\omega = 1$.

Fig. 3 depicts the threshold curves μ_{ho} for homoclinic orbits covering the range $0 < \omega < 1.6$ for different values of F. As it can be observed from this figure, as F increases the threshold μ_{ho} for the onset of chaos obtained by the Melnikov technique increases for a frequency range $0 < \omega < 1.3$.

4. Numerical simulations and analysis

In order to see the effect of the nonlinear damping in the dynamics of a particle moving in the three-well potential of our model, we have plotted the bifurcation diagram of the system Eq. (2) in the (x, b) plane for $F = 0.01$, $\mu = 0.85$, $\omega = 0.75$ with $(x_0, \dot{x}_0) = (0.1, 0.5)$ (see Fig. 4a and b). The main tool used in this investigation was a fourth-order Runge–Kutta algorithm allowing the numerical integration of model Eq. (2). The corresponding maximum Lyapunov exponent is also plotted as showed in Fig. 4c and d. From Fig. 4a, we observe that there are two different chaotic regions with period windows. Fig. 4b show the transition to chaotic region, period doubling bifurcations and period one.

The computations made to depict the complex behavior of the basin boundaries of the attraction for Eq. (2) concentrate mainly on two situations: homoclinic and heteroclinic orbits. These were done in order to support the theoretical results obtained in the previous sections. In the case of homoclinic orbit, By performing a scan of a grid 1333×833 of the initial conditions in the $(x_0, dx_0/dt)$ plane for various values of the control parameter μ. For fixed parameters $F = 0.01$ and $\omega = 1$, we find that analytical homoclinic threshold is given by $\mu \approx 0.04$ while numerical one is $\mu \approx 0.01$. The basins of attraction are regular (see Fig. 5a). As this control parameter increases above this critical value, the regular shape of basin of attraction is destroyed and the fractal behavior becomes more and more visible (see Fig. 5b–d). Such fractal boundaries indicate that whether the system is attracted to one or the other periodic attractor may be very sensitive to initial conditions. It is also found that even if μ is increased beyond the analytical critical value for the homoclinic bifurcation, it is still possible that the final steady motion could be periodic rather than chaotic. This is due to the fact that we have used the first-order approximation of Melnikov function. In the case of heteroclinic orbit, for fixing parameters $F = 0.01$ and $\omega = 0.7$, we find that analytical heteroclinic threshold is given by $\mu \approx 0.2$ while numerical one is $\mu \approx 0.07$. When μ is less than the heteroclinic critical value, the basins of attraction are regular (see Fig. 6a and b).
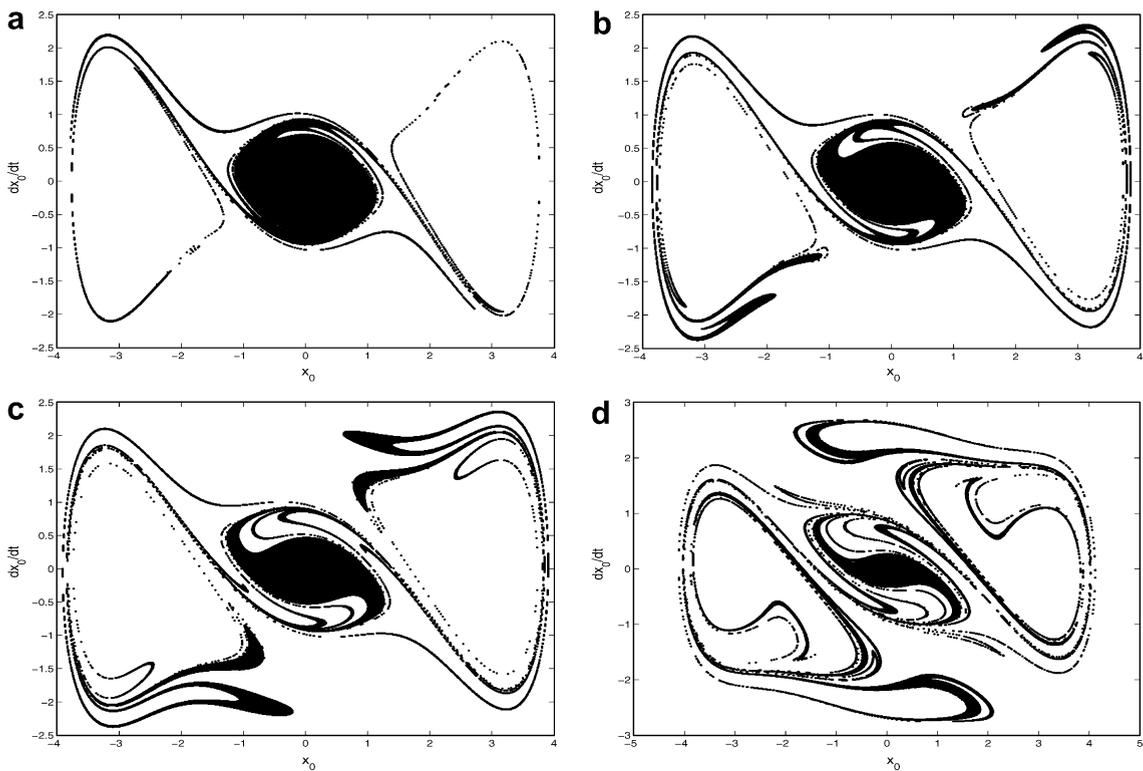

Fig. 6. Basin of attraction inside the medium potential well: (a) $\mu_{he} = 0.07$, (b) $\mu_{he} = 0.2$, (c) $\mu_{he} = 0.35$ and (d) $\mu_{he} = 0.7$, the others parameters are; $F = 0.01$, $\omega = 0.7$.

As μ increases, the regular shape of basin of attraction is destroyed and the fractal behavior becomes more and more visible (see Fig. 6c and d).

5. Conclusions

In this paper, the dynamics of a parametrically driven Extended Rayleigh Oscillator with a three-well potential has been studied. The Melnikov method has been applied when the system is perturbed to determine the threshold of homoclinic and heteroclinic bifurcations which are the "precursors" of the chaotic behaviors in the dynamical systems. Through the basin boundaries, bifurcation diagrams obtained from the direct numerical integration of the equation motion, a good agreement between the analytical estimates and the numerical observations is observed. Moreover, the effect of using the parametric perturbation on the erosion of the fractal basin boundaries has been studied. By fixing all the parameters of the system and varying only the amplitude of the parametric excitation above the critical value, the increasing amplitude of the parametric excitation provokes a rapid erosion of the basin boundaries of attraction.

Appendix A

The parameters used in the case of the heteroclinic orbit are defined as follows:

$$C_{\text{he}} = \frac{402\xi^4 + 4231\xi^3 + 5063\xi^2 + 4448\xi + 976}{3(\xi - 1)},$$

$$D_{\text{he}} = \frac{2082\xi^4 + 3696\xi^3 + 5889\xi^2 + 405\xi + 135}{3(\xi - 1)},$$

$$\eta_2 = \frac{8\pi}{15}\left(1 + \frac{\omega^2}{T_1^2}\right)\left(1 + \frac{4\omega^2}{T_1^2}\right) - 2\pi\left(1 + \frac{4\omega^2}{T_1^2}\right) + 3,$$

$$R_1 = \frac{x_1^2 T_1}{2(1 + \xi)}\left[a(\xi + 2) + \frac{bx_1^2 T_1^2 C_{\text{he}}}{160(1 + \xi)^3} + \frac{\arcsin\xi + \frac{\pi}{2}}{\sqrt{1 - \xi^2}}\left[a(1 + 2\xi) + \frac{bx_1^2 T_1^2 D_{\text{he}}}{160(1 + \xi)^3}\right]\right], \tag{14}$$

$$R_2 = \frac{4\mu x_1^2 \omega^2}{T_1^2 \sinh\frac{2\pi\omega}{T_1}}\left(2\pi + \frac{\pi\alpha x_1^2}{3}\left(5 - \frac{4\omega^2}{T_1^2}\right) + \frac{2\beta x_1^4 \eta_2}{3}\right), \tag{15}$$

$$R_3 = \frac{2\pi\omega F x_1}{T_1 \sinh\frac{\pi\omega}{T_1}}, \tag{16}$$

$$R = \frac{\pi F T_1 \sinh\frac{2\pi\omega}{T_1}}{2x_1\omega\left(2\pi + \frac{\pi\alpha x_1^2}{3}\left(5 - \frac{4\omega^2}{T_1^2}\right) + \frac{2\beta x_1^4 \eta_2}{3}\right)\sinh\frac{\pi\omega}{T_1}}. \tag{17}$$

Appendix B

The parameters used in the case of the homoclinic orbit are defined as followed

$$C_{\text{ho}} = \frac{6\xi^5 + 42\xi^4 + 603\xi^3 + 561\xi^2 + 566\xi + 112}{\xi - 1},$$

$$D_{\text{ho}} = \frac{320\xi^4 + 400\xi^3 + 765\xi^2 + 315\xi + 90}{\xi - 1},$$

$$\eta_3 = (1 - \xi)\left(1 + \frac{4\omega^2}{T_1^2}\right) + 3(1 + \xi),$$

$$\eta_4 = 8\left(1 + \frac{4\omega^2}{T_1^2}\right)\left(1 + \frac{\omega^2}{T_1^2}\right)(1 - \xi)^2 + 10(1 - \xi^2)\left(1 + \frac{4\omega^2}{T_1^2}\right) + 15(1 + \xi)^2,$$

$$K_1 = \frac{x_1^2 T_1}{4(1 + \xi)^2}\left[a(\xi^2 + 3\xi - 2) + \frac{bx_1^2 T_1^2 C_{\mathrm{ho}}}{240(1 + \xi)^2} + \frac{\arcsin \xi - \frac{\pi}{2}}{\sqrt{1 - \xi^2}}\left[a\xi(3\xi - 1) + \frac{bx_1^2 T_1^2 D_{\mathrm{ho}}}{240(1 + \xi)^2}\right]\right], \tag{18}$$

$$K_2 = \frac{2\pi\mu x_1^2 \omega}{T_1 \sinh\frac{2\pi\omega}{T_1}}\left[\frac{\sinh\left(\frac{2\omega}{T_1}\arccos \xi\right)}{\sqrt{1 - \xi^2}} + \frac{4\alpha x_1^2 \omega(1 - \xi)\eta_3}{3T_1(1 + \xi)^2} + \frac{4\beta\omega x_1^4(1 - \xi)\eta_4}{15T_1(1 + \xi)^3}\right], \tag{19}$$

$$K_3 = \frac{2Fx_1}{T_1}\sin\frac{2\omega}{T_1}, \tag{20}$$

$$K = \frac{F\sin\frac{2\omega}{T_1}\sinh\frac{2\pi\omega}{T_1}}{\pi x_1 \omega\left[\frac{\sinh\left(\frac{2\omega}{T_1}\arccos \xi\right)}{\sqrt{1 - \xi^2}} + \frac{4\alpha x_1^2 \omega(1 - \xi)\eta_3}{3T_1(1 + \xi)^2} + \frac{4\beta\omega q_1^4(1 - \xi)\eta_4}{15T_1(1 + \xi)^3}\right]}. \tag{21}$$

References

[1] Li GX, Moon FC. Criteria for chaos of a three-well potential oscillator with homoclinic and heteroclinic orbits. J Sound Vib 1990;136:17.

[2] Rajasekar S, Parthasarathy S, Lakshmanan M. Prediction of horseshoe chaos in BVP and DVP oscillators. Chaos, Solitons & Fractals 1992;2:271.

[3] Litak G, Syta A, Borowiec M. Suppression of chaos by weak resonant excitations in a non-linear oscillator with a non-symmetric potential. Chaos, Solitons & Fractals 2007;32:694.

[4] Jing Z, Huang J, Deng J. Complex dynamics in three-well Duffing system with two external forcings. Chaos, Solitons & Fractals 2007;33:795–812.

[5] Yang X, Xu W, Sun Z, Fang T. Effect of bounded noise on chaotic motion of a triple-well potential system. Chaos, Solitons & Fractals 2005;25:415.

[6] Zhang W, Yu P. A study of the limit cycles associated with a generalized codimension-3 Lienard oscillator. J Sound Vib 2000;231:145.

[7] Nayfeh AH, Mook DT. Nonlinear oscillations. John Wiley and Sons; 1979.

[8] Den Hartog JP. Mechanical vibrations. New York: Dover Publishers; 1984.

[9] Bogarcz R, Ryczek B. Dry friction self-excited vibrations, analysis and experiment. Eng Trans 1997;45:197.

[10] D'Acunto M. A simple model for low friction systems. In: Bhushan B, editors, Nato ASI Series E; 2001. p. 311.

[11] Jing Z, Yang Z, Jiang T. Complex dynamics in Duffing–Van der Pol equation. Chaos, Solitons & Fractals 2006;27:722.

[12] Minorski N. Mechanical vibratios. Warsaw: WNT; 1967.

[13] Sanjuán MAF. The effect of nonlinear damping on the universal escape oscillator. Int J Bifurcat Chaos 1999;9:735.

[14] Warminski J, Balthazar JM. Vibrations of a parametrically and self-excited system with ideal and non-ideal energy sources. J Braz Soc Mech Sci Eng 2003;25:413.

[15] Warminski J. Regular, chaotic and hyperchaotic vibrations of nonlinear systems with self, parametric and external excitations. Mech Automat Control Robot 2003;14:891.

[16] Cao H, Chen G. Global and local control of homoclinic and heteroclinic bifurcations. Int J Bifurcat Chaos 2005;15:2411.

[17] Tang Jia-Shi, Fu Wen-Bin, Li Ke-An. Bifurcations of a parametrically excited oscillator with strong nonlinearity. Chin Phys Soc 2002;11:1004.

[18] Wehrmann O. Reduction of velocity fluctuation in a Kármán vortex street by a vibrating cylinder. Phys Fluids 1965;8:760.

[19] Lima R, Pettini M. Suppression of chaos by resonant parametric perturbation. Phys Rev A 1990;41:726.

[20] Belhaq M, Houssni M. Suppression of chaos in averaged oscillator driven by external and parametric excitations. Chaos, Solitons & Fractals 2000;11:1237.

[21] Cicogna G. Changing the threshold of chaos by resonant parametric modulation. Nuovo Cim B 1990;105:813.

[22] Melnikov VK. On the stability of the center for time-periodic perturbations. Trans Moscow Math Soc 1963;12:1.

[23] Delignières D, Nourrit D, Deschamps T, Lauriot B, Caillou N. Effects of practice and task constraints on stiffness and friction functions in biological movements. Human Mov Sci 1999;18:769.

[24] Siewe MS, Moukam Kakmeni FM, Tchawoua C. Resonance oscillations and homoclinic bifurcation in a Φ^6-Van der Pol oscillators. Chaos, Solitons & Fractals 2004;21:841.

[25] Siewe MS, Moukam Kakmeni FM, Tchawoua C, Woafo P. Bifurcations and chaos in periodically and externally driven Φ^6-Van der Pol oscillators. Physica A 2005;357:383.

[26] Siewe MS, Cao H, Sanjuán MAF. Effect of nonlinear dissipation on the boundaries of basin of attraction in two-well Rayleigh-duffing oscillators. Chaos, Solitons & Fractals 2009;39:1092–9.

[27] Cao H, Seoane JM, Sanjuán MAF. Symmetry-breaking analysis for the general Helmholtz–Duffing oscillator. Chaos, Solitons & Fractals 2007;34:197–212.

[28] Sanjuán MAF. Subharmonic bifurcations in a pendulum parametrically excited by a non-harmonic perturbation. Chaos, Solitons & Fractals 1998;9:995–1003.

[29] Sanjuán MAF. Remarks on transitions order-chaos induced by the shape of the periodic excitation in a parametric pendulum. Chaos, Solitons & Fractals 1996;7:435–40.

[30] Wiggins S. Introduction to applied nonlinear dynamical systems and chaos. New York, Heidelberg, Berlin: Springer-Verlag; 1990.

[31] Trueba JL, Baltanás JP, Sanjuán MAF. A generalized perturbed pendulum. Chaos, Solitons & Fractals 2003;15:911.